Multi-Hop Conjugation Based Bacteria Nanonetworks

Sasitharan Balasubramaniam*, *Member, IEEE*, and Pietro Lio'

***Abstract*—Molecular communication is a new paradigm for nanomachines to exchange information, by utilizing biological mechanism and/or components to transfer information (e.g., molecular diffusion, neuronal networks, molecular motors). One possible approach for molecular communication is through the use of bacteria, which can act as carriers for DNA-based information, i.e., plasmids. This paper analyzes multi-hop molecular nanonetworks that utilize bacteria as a carrier. The proposed approach combines different properties of bacteria to enable multi-hop transmission, such as conjugation and chemotaxis-based motility. Various analyses have been performed, including the correlation between the success rate of plasmid delivery to the destination node, and the role of conjugation in enabling this; as well as analyses on the impact of large topology shapes (e.g., Grid, Random, and Scale-free) on the success rate of plasmid delivery for multiple source-destination nanonetworks. A further solution proposed in this paper is the application of antibiotics to act as filters on illegitimate messages that could be delivered by the bacteria. Our evaluation, which has been conducted through a series of simulations, has shown that numerous bacteria properties fit to properties required for communication networking (e.g., packet filtering, routing, addressing).**

***Index Terms*—Bacteria conjugation, bacteria nanonetworks, nano and molecular communication.**

I. Introduction

NANOTECHNOLOGY in recent years has led to the development of sophisticated devices at miniature scale. These devices have diverse capabilities ranging from encapsulations of drug molecules that can be delivered to targeted areas, all the way to nanorobots that can perform surgical tasks. However, a new and emerging research area in the field of nanotechnology is communication. Communication between the nanodevices can play a crucial contributing role that could further enhance the capabilities and functionalities of nanodevices. However, designing communication capabilities between the devices of such miniature size brings along a number of challenges. First and foremost, is the limited power such devices are envisioned to have, where embedding a dedicated communication circuitry would not be feasible. This leads to a requirement for a new communication paradigm to support the exchange of information at the nanoscale, and one approach is known as *molecular communication* [1]. In molecular communication, information is converted into molecules at the transmitting nanomachine and transported to a receiving nanomachine, which in turn decodes the information. Numerous solutions for molecular communication have been proposed including the use of molecular diffusion [27], [28] [29], calcium signaling [2], neuronal networks [3], [15] , nano arrays [14], as well as bacteria communication nanonetworks [4], [5] [11], [24]. While molecular communication is still a challenging on-going research, a paralleled area that could further improve the application base is creating networks between multiple nanomachines, i.e., *molecular nanonetworking*. In this paper, we propose one possible molecular nanonetworking solution using bacteria. Bacteria have a number of interesting characteristics that make them ideal as information carriers for nanonetworks.

This paper proposes two **design** processes for bacteria nanonetworks, which include:

1) **Bacteria conjugation**: A process that allows different bacteria to interconnect temporarily and pass copies of plasmids (genetic messages which are encoded as strings of possible four nucleotides). This process is utilized to allow different bacteria to opportunistically pass plasmids between each other. Through this opportunistic message passing, the aim is to have messages eventually arrive at the destination nanomachine. This process is also used to enable multi-hop transmission for multiple source-destination pairs. Our previous work in [5] considered this same property for only a single source-destination pair, where each bacterium can only carry a single plasmid.
2) **Antibiotic treatment**: Over the years, a number of studies have shown that bacteria are able to exhibit a certain degree of resistance to antibiotics. Based on this property, we will determine how effective antibiotics could be used to filter and kill off bacteria that do not contain legitimate plasmids (e.g., plasmids that have only gone through partial conjugation).

Thorough evaluations of the design processes will be conducted, where these evaluations include:

1) **Information theoretic analysis**: We analyze the reliability of successful plasmid transmission to a destination node (the terms node and nanomachine will be used interchangeably) for a number of small topologies. This will correlate the effect of conjugation on successful plasmid transmission, and how this correlation is affected by varying the distance parameter. This will then be followed by analyzing the noise effects through application of antibiotics, as described above.

Manuscript received May 25, 2012; revised December 14, 2012; accepted December 28, 2012. Date of publication February 06, 2013; date of current version February 27, 2013. This work was supported by the FiDiPro program of Academy of Finland "Nanocommunication Networks" 2012–2016, as well as EU FP7 FP7-HEALTH-2012-INNOVATION-Mimomics. *Asterisk indicates corresponding author.*

*S. Balasubramaniam is with the Department of Electronic and Communication Engineering, Tampere University of Technology, Tampere, Finland (e-mail: sasi.bala@tut.fi).

P. Lio' is with the Computer Laboratory, University of Cambridge, UK (e-mail: pl219@cam.ac.uk).

Color versions of one or more of the figures in this paper are available online at http://ieeexplore.ieee.org.

Digital Object Identifier 10.1109/TNB.2013.2239657

2) **Evaluation for multiple source-destination pairs**: We analyze the effects of bacteria conjugation in successfully transmitted plasmids to distant nodes within multiple source-destination pairs for different topology shapes (e.g., Grid, Random, and Scale-free).

The evaluation of our analysis will be conducted through a series of simulations.

This paper is organized as follows. Section II reviews the current related work in molecular communication, in particular focusing on bacteria nanonetworks. Section III describes the key properties of bacteria that are relevant to our proposed networking mechanisms between nanomachines. An overview of bacteria nanonetworks is provided in Section IV, which also includes the description on the concept of opportunistic routing. Section V describes the message construction using plasmids, and the use of antibiotics to improve message delivery. A description of the bacteria model and simulation design is presented in Section VI. Section VII evaluates our simulation work, and Section VIII presents a discussion on possible applications and future directions that can be taken from the proposed approach. Last, Section IX presents the conclusion.

II. Related Work

Gregori and Akyildiz [24] proposed the use of bacteria to support medium range molecular communication. The authors discussed mechanism of encoding plasmid messages, and processes for a bacterium to carry the plasmid. Cobo-Rus and Akyildiz [4] developed a simulation model for end-to-end capacity of bacteria based molecular communication. The model considers the moment when the bacteria are attracted to the source nanomachine, latch on the nanomachine to retrieve the DNA strands, propagate to the destination, and finally unload the message plasmid at the receiving nanomachine. The evaluation also includes the propagation delay and distance travelled by the bacterium to get to the receiver, depending on the quantity of chemoattractant, and distances between the nanomachines. The authors also discussed mechanisms of designing the DNA strands to include information on the transfer, routing, as well as the message itself. Gehring *et al.* [8] investigated the effects that antibiotics have on a population of bacteria as they conjugate and pass on resistance genes between each other. The aim of the study is to determine the optimal antibiotics that will be required in order to minimize resistance transmission between the bacteria. The authors developed a simulation study in which bacterial populations are distributed based on a number of network topologies (including Internet service provider (ISP) network topologies, e.g., Abiliene). Gao *et al.* [9] investigated the proximity of nanomachines between each other (where each has different chemoattractants), and how this affects the performance of bacteria delay as they migrate between the nanomachines. This provides new insights into how scheduling between links can be performed for bacteria nanonetworks. Dubey and Ben-Yehuda [12] proposed nanotubes as a major form of communication between bacteria. The study is based on *Bacillus subtilis*, where nanotubes joining the bacteria were demonstrated to transfer fluorescent molecules.

While a number of different works have investigated various aspects of bacteria communication, there are no works that have investigated how multi-hop routing can be performed between different nanomachines, in particular for large-scale topologies. Our approach in this paper, however, combines a number of different elements from the works described above, and it is proposed to analyze molecular nanonetworking that can be achieved using bacteria.

III. Characteristics of Bacteria

This section will outline key characteristics and properties of bacteria, which we will use in our multi-hop routing.

A. Message Plasmids

The messages are loaded in the bacteria through coding of the plasmids [4], [24] . Plasmids are circular DNA molecules that are separate from chromosomal DNA. The plasmids can be transferred from one bacteria to the next through the conjugation process, which is described below. The plasmids can be up to *1.6 mega base pairs (mbp)* [4] long, and the conjugation process can at times transfer only a portion of the plasmids. The plasmids are built from nucleotides, which contain one of four bases. These bases include: *adenine (A), guanine (G), cytosine (C), and thymine (T)*. In later sections, we will describe how to encode our information into a plasmid, and perform watermarking process in encoding common English words into genetic code that can be inserted into the plasmids.

B. Antibiotics Effects

A number of researchers today has focused on the use of antibiotics as a mechanism to curtail the growth of bacteria, as well as to kill them. Antibiotics can eliminate bacteria in a number of ways, where these include interference with cell wall synthesis, inhibition of metabolic pathways or protein synthesis, interference with the nucleic acid synthesis, or disruption of the bacterial membrane structure [8]. Bacteria have often responded by developing genes that counteract the effects of antibiotics. These resistance genes are often contained in plasmids they exchange. The resistance genes can protect the bacteria in the form of production of enzymes that destroy the drug or modify the metabolic pathways that overcome the effects of the antibiotics. Using this type of selection (presence of the antibiotic in the medium) and counter selection (presence of the antibiotic resistance gene in the plasmid) we can eliminate bacteria not carrying an initial message, to avoid the presence of unwanted bacteria that could interfere with the routing communication, i.e., the level of noise. Therefore, antibiotics can be embedded into the nanomachines in order to eliminate noise.

In the preparatory stage, the antibiotics we want to use to clear up the bacteria not carrying a plasmid with the message could be tested using the *Kirby-Bauer disk-diffusion* method [25]. The antibiotic is impregnated in circular wafers; bacteria is grown on a plate of agar and the circular wafers are placed throughout the plate. If bacteria are not carrying resistance genes after an incubation period, a clear area around the zone of antibiotic inhibition will appear. However, bacteria that contain antibiotic

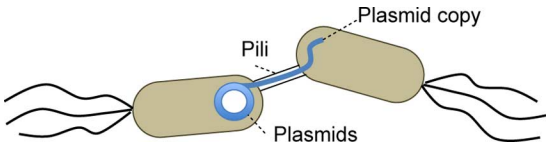

Fig. 1. Illustration of conjugation process between two bacteria. The conjugation starts with pili connections between the bacteria, before the plasmid is transferred through the connection.

resistance genes would enable normal or near normal bacterial growth.

C. Bacteria Motility

Bacteria motility is based on gliding (low speed) or flagellated motion. Bacteria can reach speeds from 2 μm/s (for example *Beggiatoa*, a gliding bacteria) to 200 μm/s (*Vibrio Cholerae*). Other examples of bacteria swimming speed includes: *Salmonella typhimurium*—20 μm/s and *Spirillum sp*—50 μm/s. Bacteria posses a sensing and motility coupled process known as *chemotaxis*, where a bacterium detect specific type of chemoattractant gradient within the environment and use this to direct themselves towards the destination. The motility process is a cycle of run and tumble phases, and the frequency of each depends on the gradient of chemoattractant sensed by the bacterium. When there is no chemoattractant, the bacterium mobilizes by random walk. However, once the bacterium is in the chemoattractant field, it will exhibit a biased random walk behavior, where the lengths of run will be longer as the strength of the chemoattractant field gets stronger. The longer running lengths will lead to less tumbling.

D. Conjugation Process

Bacterial conjugation involves the transfer of a plasmid between donor and recipient bacteria that are normally in close contact. Fig. 1 presents an example of conjugation between two bacteria. Before a conjugation process can take place, specific genes that trigger the conjugation process must first be expressed. Genetic transfer is operated by a protein complex called type IV secretion systems, which forms the *transferosome*. Before the transferosome transports the plasmid between cells, the plasmid needs to be prepared by another complex called a *relaxosome*. The relaxosome makes a cut at a precise position of the plasmid sequence called *origin of Transfer* (known as *oriT)*.

When in close proximity, the bacterium attracts another bacterium by joining the pili, and the plasmid is passed through the pili connection. In situations where the donor bacterium is close to a cluster or community of potential recipients, the process is much more efficient than by random encounters between individual bacteria. An example of a cluster or community is a chain structure, where Grossman *et al.* [7] found that certain types of plasmids such as the *ICEBs1* spread rapidly from bacterium to bacterium within the chain. This quick sequential conjugation event leads to a rapid amplification of the number of bacteria containing the genetic information that is encoded in the plasmid.

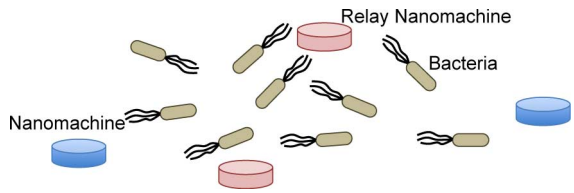

Fig. 2. Bacteria communication nanonetwork (blue nodes are source and destination nodes, while pink nodes are relay nodes).

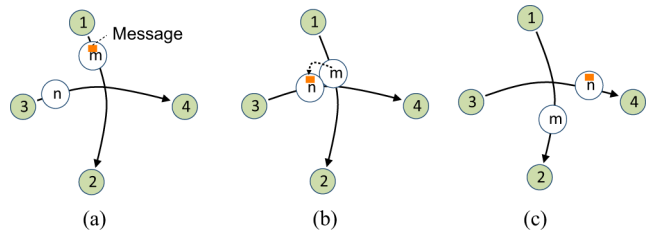

Fig. 3. Example of DTN based opportunistic routing for mobile wireless networks. The message originated from node 1, carried by mobile device m, which is opportunistically passed to mobile device n.

IV. Bacteria Communication Nanonetworks

A typical bacteria communication nanonetwork is illustrated in Fig. 2. The scenario of our bacteria communication nanonetwork is an environment that consists of nanomachines, where our aim is to allow the nanomachines to communicate with each other. Each nanomachine is assumed to be able to emit a chemoattractant that attracts the bacteria. Therefore, as illustrated in Fig. 2, the information will be delivered through bacteria that swim within the environment.

The aim of developing multi-hop routing in bacteria nano networks is motivated by a number of reasons, including the need to ensure, i) reliability in transmission between distance nanomachines, and ii) that multiple source-destination nanonetworking can be performed. The case of i) and ii) will play a major role, since bacteria will only have limited spatial mobility capabilities, depending on the chemoattractant concentration within the environment. Therefore, intermediate nanomachines can be used as relay nodes that attract certain bacteria to migrate to specific positions, therefore behaving as bacteria relay carrier. The following subsection will introduce the concept of *Opportunistic Routing*, which we propose as a routing mechanism for bacteria nanonetworks.

A. Opportunistic Routing

Opportunistic Routing is a routing process that is usually applied to wireless networks. The concept basically relies on intermediate nodes that have good immediate link qualities to forward packets to a destination node, in the event that the source to destination node link is poor or not within range. One form of opportunistic routing is based on the concept of *Delay Tolerant Networking (DTN)* [17], [18] . In DTN, mobile nodes opportunistically meet and pass messages to each other, where eventually this message will reach the destination point. An example of DTN based opportunistic routing is illustrated in Fig. 3, where mobile device m is traveling from node 1 to 2, and mobile device n is traveling from node 3 to 4. Through their mobility paths, the two nodes come into close proximity, providing an opportunity for node m to offload a message to n. This in turn

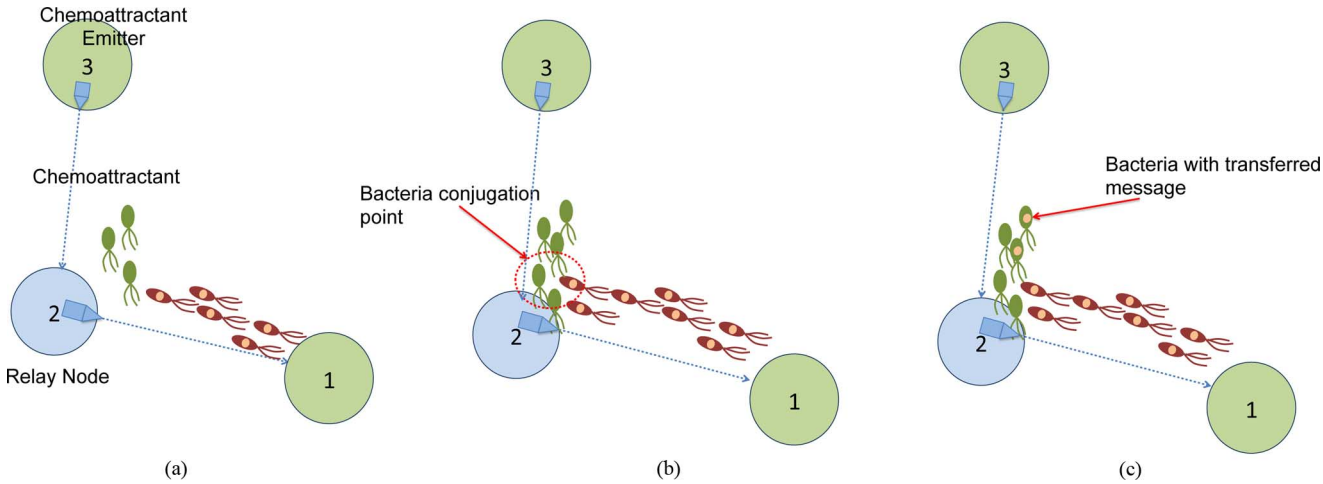

Fig. 4. Illustration of conjugation based routing for bacteria nanonetworks. The source node is node 1 and the destination node is node 3. In this example, the red bacteria are attracted to the chemoattractant from node 2, while green bacteria are attracted to node 3. The mobility of the two different groups of bacteria will lead to opportunistic conjugation, enabling message plasmids to finally arrive at node 3.

will allow the message to be transmitted from node 1 to node 4 without a preset routing table.

B. Conjugation Based Opportunistic Routing

The process for multi-hop routing in bacteria nanonetworks is through the combined process of conjugation and chemotaxis [5] as shown in the example in Fig. 4. Our approach is similar to wireless broadcast networks, where messages that are intended for specific recipient nodes will be received, while messages not intended for the recipients will be dropped. Similar to the example in Fig. 3, in this example, node 1 wants to transmit a message to node 3, by using the relay node 2. The chemoattractant from node 2 will attract bacteria traveling from node 1, while the chemoattractant from node 3 will attract bacteria from node 2. As the two groups of bacteria approach each other, a conjugation process occurs, leading to messages of bacteria from node 1 to conjugate with bacteria from node 2. Eventually, the message will be transmitted to the destination node 3.

The delay for message transmission from a source node to a destination node that goes through N conjugations, can be represented as

$$t_{end\text{-}to\text{-}end,N} = t_{encoding}(plas) + t_{decoding}(plas) + t_{delivery}(plas, N) \quad (1)$$

where $plas$ is the plasmid. The $t_{encoding}(plas)$ will depend on the time to encode the plasmid, as well as the time for the bacterium to latch to the nanomachine to retrieve the plasmid, while the $t_{decoding}(plas)$ will depend on the time for the bacterium to latch to the receiver nanomachine to offload the plasmid. The time for encoding ($t_{encoding}(plas)$) the plasmid could be based on the solution proposed by [4]. The latching time at the source and receiver nanomachines is defined as the time taken for conjugation (t_{conj}). In this paper, we will only concentrate on the $t_{delivery}(plas)$, where

$$t_{delivery}(plas, N) = \sum_{i}^{N} t_{conj,i}(plas) + \sum_{i}^{N} t_{prop,i}. \quad (2)$$

This is represented for a plasmid $plas$ that has gone through N number of conjugations. The breakdown of the $t_{delivery}$ is as follows:

- $t_{conj,i}(plas)$ represents the conjugation time for bacterium i, where

$$t_{conj,i}(plas) = t_{pili_{form},i} + t_{trans,i \longrightarrow j} \quad (3)$$

- $t_{pili_{form},i}$ represents the time for the pili on the bacterium to be formed.
- $t_{trans,i \longrightarrow j}$ is the time required for the message to be transferred between bacteria i and j during the conjugation process. We assume the speed to be 833 bp/s [4].
- $t_{prop,i}$ represents the propagation time of bacterium i.

V. Plasmid Construction

A. Message Construction

The conjugation process as described above is performed in a particular sequence, whereby the transfer will start at a specific position and slowly pass the entire sequence through to the receiving bacterium. This is illustrated in Fig. 5, where we can see that the origin of the message is at the beginning of the sequence. Our intention is to have a process whereby complete messages could be successfully transferred to the destination node. To ensure this, we have placed a resistant gene in the plasmid. The resistant gene allows bacteria to be resistant to antibiotics. Therefore, as shown in the figure, the placement of the resistant gene is important to ensure that the maximum amount of the message is transferred over. In this particular case, we have inserted the resistance gene at the end of the message. This means, that in the event of a conjugation process that is not fully successful, only a portion of the message would be transferred through, and it would miss out on the resistance gene. Therefore, the antibiotics will kill this particular bacterium, since only a portion of the message was successfully passed through. However, if the conjugation process is performed past the resistance gene, then

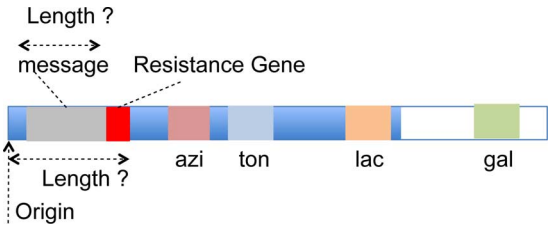

Fig. 5. An example illustration of inserting a message with a resistance gene into a plasmid (azi, ton, lac, gal are other types of genes).

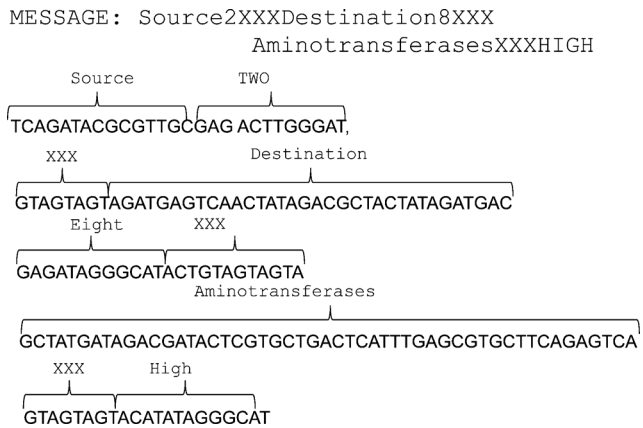

Fig. 6. Example of coding english messages for plasmids into nucleotide bases using watermarking.

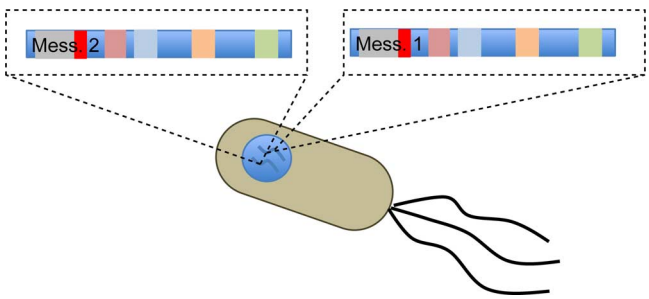

Fig. 7. Illustration of bacteria with multiple plasmid messages.

the inherited resistance gene will allow the bacterium to survive.

Messages could be encoded using a type of watermaking such as that used by Venter *et al.* [16]. As an example, we take a message that is sent and coded by a nanomachine, where this message and its plasmid sequence is shown in Fig. 6. Fig. 7 illustrates a bacterium that is able to hold multiple plasmids. This process usually occurs as a bacterium encounters multiple conjugation processes, leading to multiple plasmid messages. By having bacteria that can carry multiple plasmids, will lead to multiple message transmissions from various sources to a destination node. This in turn increases the likelihood of message delivery to a destination nanomachine. The messages will contain the address of the destination node, and we assume that each nanomachine has the ability to read and interpret the addresses. If the recipient recognizes the address as its own, the message is received, else the message is eliminated.

VI. Bacteria Model and Simulation Design

The parameters used for our bacterium model is presented in Table I. The simulated motility model of our bacterium is based on a biased random walk, as proposed by [10], and illustrated

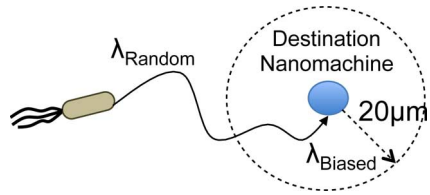

Fig. 8. $E.$coli motility simulation model. When the bacterium is in a chemoattractant free environment, the bacterium running time is governed by exponential distribution with λ_{Random}. However, once the bacterium senses chemoattractant in the environment, the bacterium running time is governed by exponential distribution with λ_{Biased}.

TABLE I
Bacteria Motility Parameters

Parameter	Value
Bacterium size	2 μm long; 1 μm wide
Speed	20 μs
Run duration towards dest.	Exponential distribution (λ_{biased})
Run duration away from dest.	Exponential distribution (λ = 1/3.5)
Tumbling angle	Normal distribution [0, 2π)
Direction of Tumbling	Bernoulli
Number of chemoattactants	1/bacteria
Conjugation time (T_{CONJ})	Uniform Distribution (0-1800s)
Message length	1000Kbp
Transfer speed	833bp/s
Message threshold	300s
Max. plasmids/bacteria	10
Conjugation Probability	0.5

TABLE II
Nanomachine Parameters

Parameter	Value
No. of chemoattractant/node	2 - 4
Receiver radius	2 μm
Number of bacteria caged in each node	(2 - 40)
Diameter of Emission	20 μm
Diffusion coefficient (D)	10^{-9} m^2/s
Attractant emission rate (Q)	10^{-11} mol/s

in Fig. 8. As described earlier, the motility of the bacterium is based on the quantity of chemoattractant sensed in the environment. In the event the bacterium is outside the chemoattractant range, the bacterium moves through a random walk, and will tumble often. However, once the bacterium enters the chemoattractant field, the running period is longer. Therefore, for the random walk, the running period is determined by an exponential distribution with a fixed λ. However, once the bacterium enters the chemoattractant zone, the running time varies depending on the sensed quantity of chemoattractant. In this situation, the running period is determined by an exponential distribution with a varying λ_{Biased}, which is represented as

$$\lambda_{Biased} = \log 1.6 D_{Bac} E_r + 1. \quad (4)$$

For the λ_{Biased}, D_{Bac} represents the current distance of the bacterium to the destination node, and E_r is the emission radius of the chemoattractant.

We model the movement of the bacterium along a two dimensional $x - y$ grid. After Δt, the bacterium will be displaced to position (x_i, y_i), and the displacement is represented as

$$x_i = x_{i-1} + (R_T S_b A_x) \quad (5)$$
$$y_i = y_{i-1} + (R_T S_b A_y) \quad (6)$$

TABLE III
COMPARISON OF SINGLE HOP TO MULTI-HOP

Type	Mean No. of Messages	STD	Mean Time of 1st Message Arrival (s)	STD
Single	0.02	0.14	299.96	2557.91
Multi	0.21	0.41	34621.5	86246.8

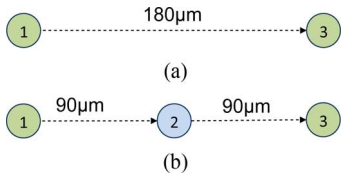

Fig. 9. (a) Single-hop transmission, (b) 2 node multi-hop transmission.

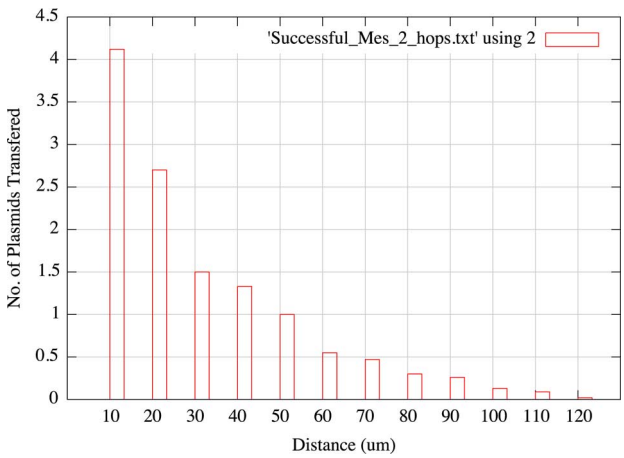

Fig. 10. Distribution of successful messages arriving at destination with respect to varying distance for single-hop.

where

$$A_x = \begin{cases} \cos\theta_k & \text{if } 90 < \theta_k < 180;\ 270 < \theta_k < 360 \\ \sin\theta_k & \text{if } 0 < \theta_k < 90;\ 180 < \theta_k < 270 \end{cases} \quad (7)$$

$$A_y = \begin{cases} \sin\theta_k & \text{if } 90 < \theta_k < 180;\ 270 < \theta_k < 360 \\ \cos\theta_k & \text{if } 0 < \theta_k < 90;\ 180 < \theta_k < 270. \end{cases} \quad (8)$$

Therefore, the value of A_x is highly dependent on θ_k, which is the angle resulting from the tumbling process. As presented in Table II, the value of θ_k is an independent, identical random variable from the previous value and is represented as a uniform distribution. However, before the value of θ_k is selected, the direction of tumbling is first determined, and this is based on a Bernoulli trial [10].

In our simulation we assume a steady state chemoattractant field, that is represented as [4]

$$U(r,t) = \frac{1}{1000}\frac{Q}{4D\pi r} \quad (9)$$

where D is the diffusion coefficient of the chemoattractant, r is the radius to the center of the release point, and Q is the attractant emission rate (values are presented in Table II). As described in Section III-C, before a conjugation process the bacterium will first need to create the pili, where the pili connection between the two bacteria will be used to pass the plasmid. In our simulation, we assume that bacteria are kept in a transfer *mood* through pheromones in the medium, which means that we eliminate the time for the pili to form $(t_{pili_{form}})$ from (3) before the bacteria is ready for conjugation. The conjugation process is based on two bacteria that are found on the same grid points within the simulation space.

VII. SIMULATION

We assume in our simulation setup that bacteria are initially caged within the nanomachine, and are all released simultaneously; a similar setup to what we had proposed earlier in [5]. After a short period the bacteria will have random positions in the simulation space.

A. Comparison of Multi-hop To Single-hop

This section presents an evaluation comparison between single and multi-hop bacteria nanonetworks. The simulation running time is 40 000 s, and the results presented are for 50 simulation runs, with 30 bacteria emitted per chemoattractant link. Firstly, Fig. 10 presents the number of plasmids that reach the destination for a single-hop, as we vary the distance between the nodes. As shown in the figure, the behavior is based on a negative exponential curve as the distance increases. Table III presents the performance comparison between single-hop and multi-hop transmission for the topologies of Fig. 9. As shown in the results, the average number of successful messages reaching the destination is increased with the 2 node multi-hop topology (0.21 compared to 0.02). While the time for the 1st message to arrive is shorter in the single hop case, this is due to the long conjugation time (t_{conj}) that slows the messages in the multi-hop case.

B. Correlation Analysis

In this section, we will analyze the correlation between number of plasmids that reach the destination as well as the conjugation process for varying distances. Our aim is to analyze spatial distance changes in the topology, and how conjugation relates to the uncertainty in plasmids reaching the destination. Information theoretic analysis has been applied to quantify the importance as well as relationships between different attributes and its impact on the outcome. In this paper, we also use concepts from information theory to quantify the effects and relationships between the conjugation process (or relaying process), and success of probability of messages arriving at the destination. The justification for using information theoretic measures is because of the nature of information propagation between the source and destination points. First and foremost, the messages could get distorted during the conjugation process. Secondly, due to the random motility of bacteria, the messages may get lost during propagation. We want to determine how these factors affect the different topology shapes and types when it comes to the message successful transmission to the destination (e.g., for certain topology types, the concentration of the relay nodes may be higher in some regions with respect

to others. The direction of the chemoattractants may also impact on the diversity of migration that bacteria may take). The entropy is represented as

$$H(X) = -\sum_{x=0,1} P(X=x)\log_2 P(X=x) \tag{10}$$

$$H(Y) = -\sum_{y=0,1} P(Y=y)\log_2 P(Y=y) \tag{11}$$

while mutual information is represented as

$$I(X:Y) = \sum_{X,Y} P(X=x, Y=y) \times \log_2 \frac{P(X=x, Y=y)}{P(X=x)P(Y=y)}. \tag{12}$$

Based on this, the entropy correlation $\rho(xy)$ is represented as

$$\rho(xy) = \sqrt{\frac{2I(X:Y)}{H(X)+H(Y)}}. \tag{13}$$

Here $x = (x_o, x_1)$ represents a plasmid successfully traversing from a source nanomachine to a destination nanomachine, while $y = (y_o, y_1)$ represents a message that has successfully conjugated (successful conjugation means that the entire message was copied to the recipient bacterium). Therefore, the probability of successful message delivery to the destination node, $P(x)$, is represented as,

$$P(x = x_1) = \frac{x_1}{\sum B_{num}} \tag{14}$$

where B_{num} is the total number of bacteria in the nanonetwork. The probability of a successful conjugation process, $P(y)$, is represented as,

$$P(y = y_1) = \frac{C_{succ}}{\sum C_{total}} \tag{15}$$

where C_{succ} are the number of successful conjugation, while C_{total} is the total number of conjugations. Therefore, $1-P(y)$ is the probability that a failed conjugation process occurred. Based on this,

$$P(x = x_0) = 1 - P(x = x_1) \tag{16}$$

$$P(y = y_0) = 1 - P(y = y_1). \tag{17}$$

The probability $P = (x = x_1,\ y = y_1)$ represents the message successfully reaching a destination node, where this message has been conjugated through bacteria from intermediate relay nodes. Therefore,

$$P(x = x_0, y = y_1) = 1 - P(x = x_1, y = y_1). \tag{18}$$

The probability $P(x = x_0,\ y = y_0)$, therefore, is the cumulative probabilities that messages did not reach the destination and as well did not go through conjugation.

Fig. 12 presents the results of the correlation analysis for the three small topologies from Fig. 11. Fig. 12(a)–12(c) correspond to Fig. 11(a) (Line topology—including a broken link between nodes 2 and 3), Fig. 12(d)–12(f) correspond to Fig. 11(b) (5-node topology), while Fig. 12(g)–12(i) correspond to Fig. 11(c) (Hexagon topology). The simulation duration was for 20 000 s, and in total there were 50 simulation runs for each topology. The aim of the analysis is to investigate the plasmid delivery mechanism for small scale topologies, with varying properties (e.g., broken links, disjoint connections, multiple alternative paths), where this is used to analyze the simulation of larger topologies that will be presented in the following section. For each simulation, we have varied the amount of bacteria (20 and 30 bacteria/chemoattractant link), as well as distances, d_{nodes}, between the nodes. The number of bacteria/chemoattractant link refers to the number of bacteria emitted from a node that is attracted to the neighboring node. This is represented as an arrow indicating the direction of the chemoattractant gradient. For example in Fig. 11(a), there is a single dash line between the nodes indicating that all the bacteria are attracted to the chemoattractant from the neighboring node (single link). We assume an equal horizontal distance d_{nodes} between the nodes, as shown in the figure. The analysis includes: i) the correlation between x and y for the different types of topologies, ii) the probability of successful plasmids that have gone through conjugations, $P(x = 1,\ y = 1)$, and iii) number of successful plasmids that reach the destination (please note for each topology, the source node is 1 and destination node is 4). As expected, the correlation $\rho(xy)$ for the Line topology [Fig. 12(a)] drops as the distance d_{nodes} increase. As we increase the distance d_{nodes}, the bacteria will be out of range from the chemoattractant and would only be performing a random walk. In particular, as distance d_{nodes} increases over 20 μm, the bacteria will sense very small quantity of the chemoattractant. An interesting result is the difference between 20 and 30 bacteria/chemoattractant link, where the 30 bacteria/chemoattractant link shows a lower correlation $\rho(xy)$. This is also a similar trend found in the correlation $\rho(xy)$ of the 5-node topology in Fig. 12(d), as well as the Hexagon topology in Fig. 12(c). The main factor behind this trend is due to the same simulation time performed for both the 20 and 30 bacteria/chemoattractant link. However, in the case of 30 bacteria/chemoattractant link, due to the higher number of bacteria, this will also lead to higher probability of conjugation (and possibly multiple conjugations). Since conjugation can

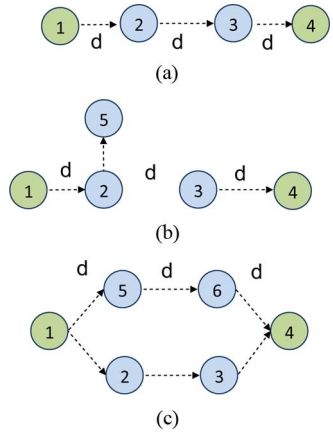

Fig. 11. (a) Line topology, (b) 5-node topology, (c) Hexagon topology. For all nodes, the source node is 1 and destination node is 4.

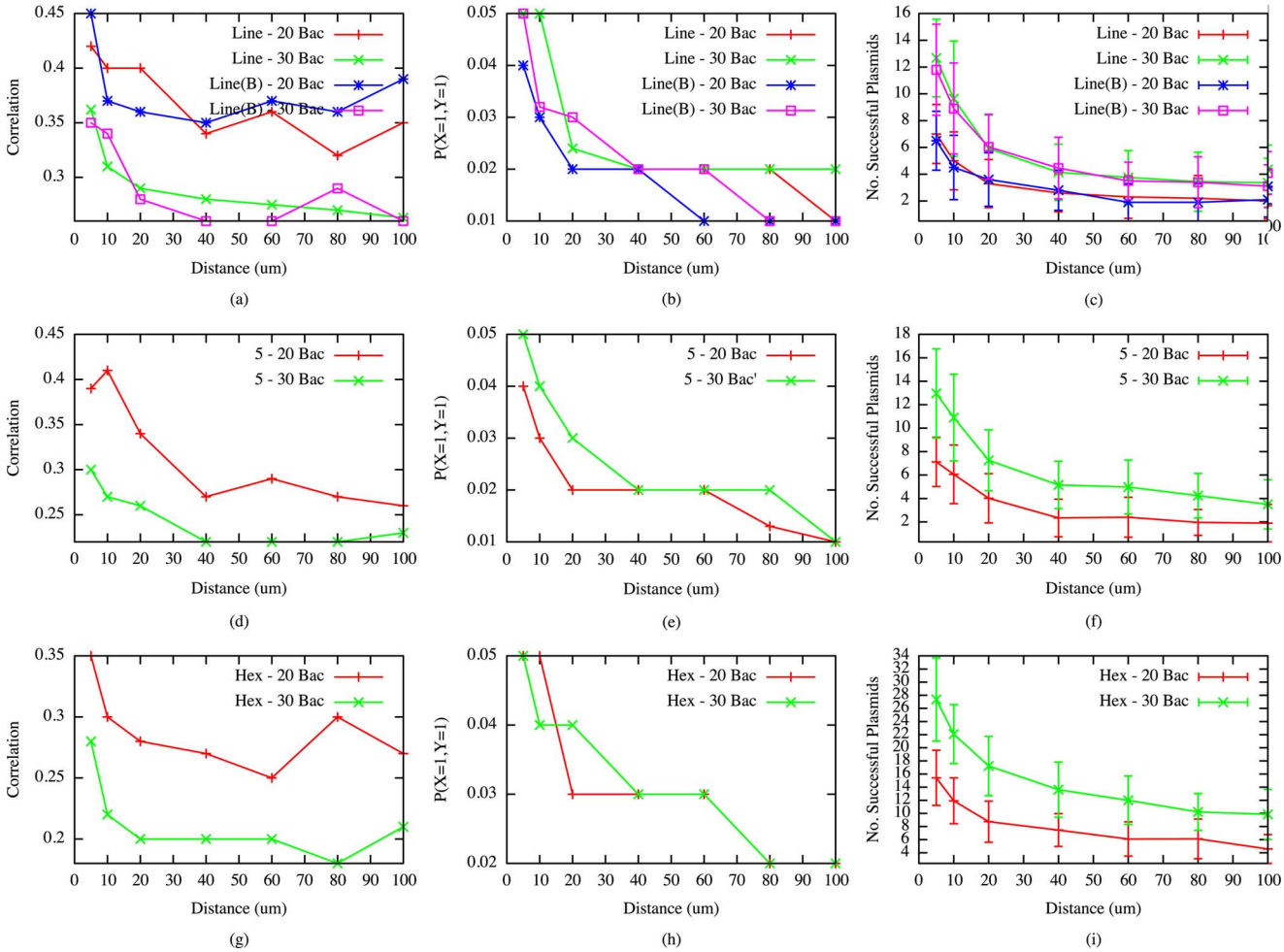

Fig. 12. (a) Entropy correlation for the Line topology (including broken link), (b) $P(x = 1,\ y = 1)$ for the Line topology (including broken link), (c) Number of successful plasmids for the Line topology (including broken link), (d) Entropy correlation for the 5-node topology, (e) $P(x = 1,\ y = 1)$ for the 5-node topology, (f) Number of successful plasmids for the 5-node topology, (g) Entropy correlation for the Hexagon topology, (h) $P(x = 1,\ y = 1)$ for the Hexagon topology, (i) Number of successful plasmids for the Hexagon topology.

take a long duration, this delays the average time bacteria needs to get to the destination point, leading to lower probability $P(x)$. An interesting result is the difference between the Line topology with perfect chemoattractant links and the broken chemoattractant link. The result shows a higher $\rho(xy)$ for the full chemoattractant links compared to the broken link for distances below 20 μm. This is due to the weak chemoattractant field that is higher than a distance of 20 μm. The drop in correlation $\rho(xy)$ is also reflected in the downtrend of probability $P(x = 1,\ y = 1)$ for the Line topology [Fig. 12(b)], 5-node topology [Fig. 12(e)], and Hexagon topology [Fig. 12(h)]. For all topologies, a large drop can be seen up to distance d_{nodes} of 20 μm, and this stabilizes on average over the distance d_{nodes} of 20 μm demonstrating that the random walk plays an equal role for all distance d_{nodes} above 20 μm. On average the number of successful plasmids reaching the destination follows a similar trend, with the 30 bacteria/chemoattractant link leading to a higher number compared to 20 bacteria/chemoattractant link. The directionality of the relay nodes towards the destination plays a crucial role in the correlation $\rho(xy)$ as well. In the case of the Line and 5-node topologies, the difference is in node 5 placement, being far from node 3. Therefore, only a small portion of bacteria from node 2 (and possibly node 5) would flow towards node 3 for the 5-node topology (we refer to this as leakage). This has resulted in a drop in correlation $\rho(xy)$ over distance d_{nodes} of 20 μm for the 5-node topology. The success rate of plasmids of the 5-node topology [Fig. 12(f)] is very similar to the Line topology [Fig. 12(c)], and this is attributed to the higher number of bacteria that the 5-node topology will have compared to the Line topology. The Hexagon topology shows a higher number of plasmids arriving at the destination compared to both the 5-node and Line topology, as shown in Fig. 12(i), compared to Fig. 12(f) and 12(c). First, the main reason for this is that in the Hexagon topology we will have two paths for the bacteria to take towards the destination (paths 1–2—3–4 and 1 –5—6–4). This in turn leads to a higher number of conjugations, that would occur along each path. Second, there are also higher number of bacteria leaving from node 1. The probability $P(x = 1,\ y = 1)$ also demonstrates this, as we can see in Fig. 12(h), compared to Fig. 12(e) and 12(b), where for the Line topology, the probability $P(x = 1,\ y = 1)$ would stabilize at 0.02 on average for distances between 20 μm $-$ 80 μm, while for the Hexagon topology we will see this stabilize at around 0.03 for distances between 40 μm $-$ 60 μm.

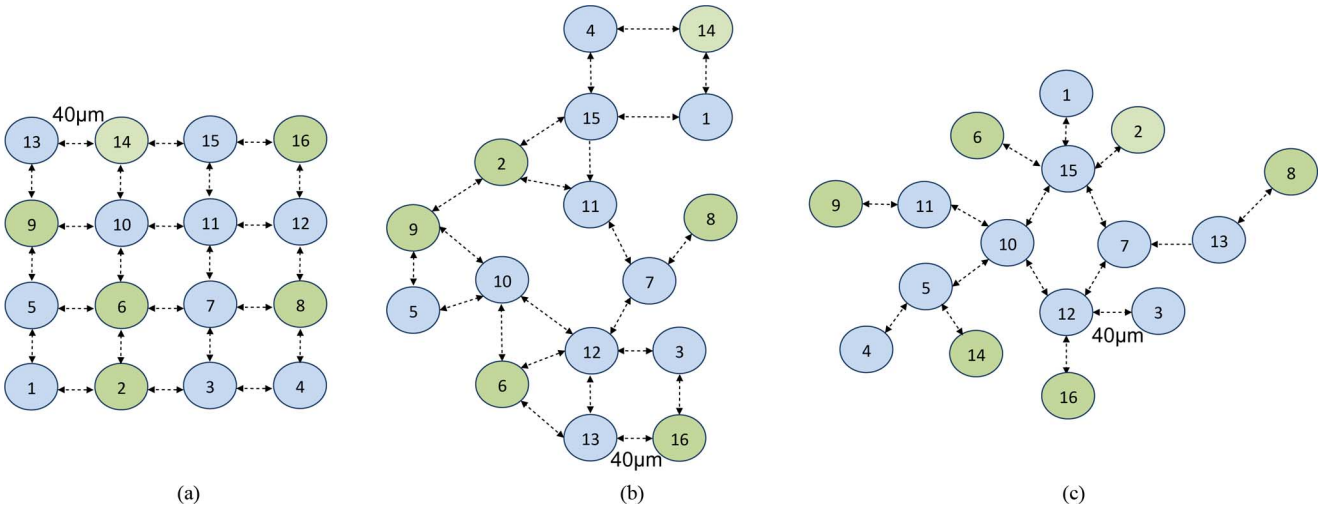

Fig. 13. (a) Grid Topology (16 node, 48 chemoattractant links), (b) Random Topology (16 node, 44 chemoattractant links), (c) Scale-free Topology (16 node, 32 chemoattractant links. For all topologies, the source nodes emitting bacteria with message plasmids are (9, 14, 8) and the destination nodes are (16, 2, 6). Each source node can transmit to all destination nodes.

C. Multiple Source-Destination Analysis

This section discusses the message delivery success rate through the combined process of chemotaxis and conjugation for bacteria nanonetworks in larger topologies, and with multiple source-destination nodes. The different topologies that we have considered in our simulations are presented in Fig. 13, which includes a Grid topology [Fig. 13(a)], Random topology [Fig. 13(b)], and Scale-free topology [Fig. 13(c)]. In the case of Grid topology there are 48 links, for Random there are 44 links, and for Scale-free topology there are 32 links. For each topology, the destination nodes are 9, 14, 8 and the source nodes are 16, 2, 6. The total simulation time is for 5000 s. For the simulation of this section, we have allocated a fixed distance d_{nodes} between the nodes, as illustrated in Fig. 13.

In order to further illustrate the combination of various processes (e.g., conjugation, antibiotics treatment), Fig. 14 presents the various processes with respect to time for a single simulation cycle. Fig. 14(a)–14(c) presents the plasmid arrival time for each topology. The blue stars indicate the time a conjugation process occurred, and the pink stars represents the bacteria killed by antibiotics. Fig. 14(c)–14(f) shows the number of message plasmids that arrived with respect to the originating source node, while Fig. 14(g)–14(i) shows the number of message plasmids that arrived at specific destination node. In our simulation, we assume that each source can transmit to any destination. The Grid topology [Fig. 14(a), 14(d), 14(g)], shows a high number of conjugation processes occurring. This is reflected from the high connectivity of the Grid topology, which leads to a higher number of bacteria, as described earlier. Fig. 14(d) shows that at each time interval, messages will arrive at each destination, and this drops to an average of two destinations after 2500 s. The majority of the messages at the latter part of the simulation are from conjugation, where bacteria will carry more than two messages. Fig. 14(g) also shows that originating sources of plasmids are equally distributed throughout the simulation duration. The number of conjugation processes is lower in the Random topology [Fig. 14(b)], and we see in Fig. 14(e) that first half of the time interval will have plasmids arriving at all destinations. This is due to a number of factors including lower number of backup paths compared to the Grid topology (which we have shown leading to a higher impact in the previous section of the Hexagon topology). An interesting behavior is at time 1500 s, which shows the highest number of plasmids arriving at the destination. This means that the conjugation process has resulted in a number of bacteria containing a certain number of plasmids, increasing the number of plasmids arriving at the destination. The Scale-free topology on the other hand shows very sparse and low number of conjugations occurring, at the central period of the simulation [Fig. 14(c)]. Fig. 14(f) also shows that the majority of the time intervals only led to maximum two destination nodes picking up new plasmid messages, and this is also reflected in the number of sources where the messages originated from [Fig. 14(i)]. This is reflected by a number of reasons. Firstly, compared to the Grid topology, there is a very limited number of back-up paths. In the case of Scale-free topology, only limited number of nodes act as central relay for the entire topology, and these nodes are 10, 15, 12, 7. In a number of cases, the bacteria would flow directly to the destination node if they are in close proximity. For example, bacteria from node 14 can flow directly to node 16. A similar case can be found for bacteria flowing from node 8 to node 2, but taking a longer period (hence, the majority of bacteria arriving at time interval 1000 s). However, the conjugation process does play a role, but towards the end of the simulation at time 5000 s, and this is due to the lesser amount of bacteria, as well as minimum back-up paths.

Fig. 15 presents the results on the successful plasmids reaching the destination as we vary the number of bacteria/chemoattractant links. As shown in the results, the number of successful plasmids reaching the destination grows linearly as we increase the number of bacteria/chemoattractant link. The best results is from the Grid topology, followed by the Random topology, and lastly the Scale-free topology. In the case of the highest number of bacteria/chemoattractant links (e.g., 10 bacteria/link), for Grid topology we are able to achieve up to 50 plasmids reaching the destination, compared to 26 for Random

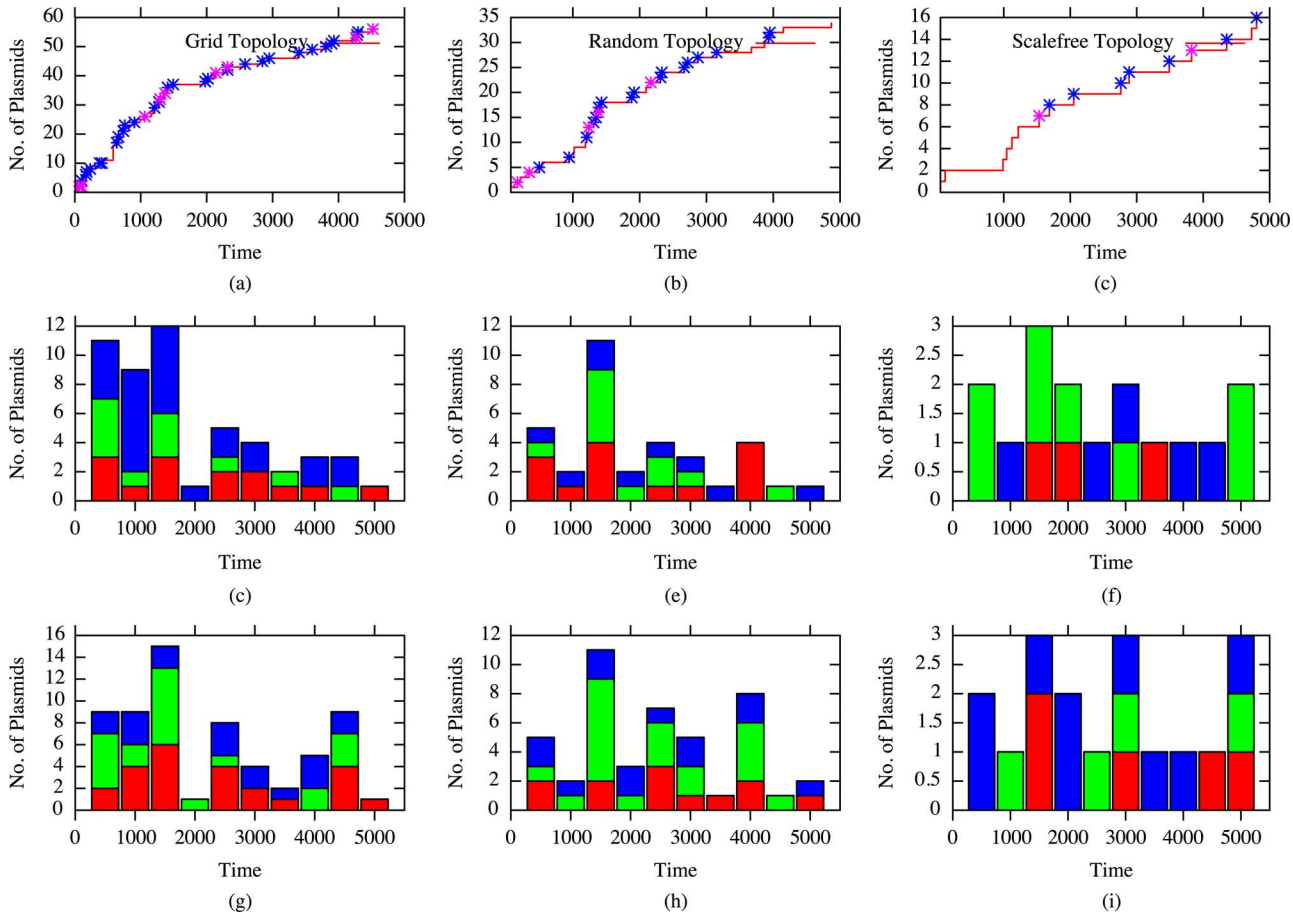

Fig. 14. Single simulation run to illustrate combined processes of conjugation and antibiotics treatment with respect to time, (a) Bacteria arrival with respect to time for the Grid topology, (b) Bacteria arrival with respect to time for the Random topology, (c) Bacteria arrival with respect to time for the Scale-free topology, (d) Number of messages arrived to each destination for the Grid topology (*blue is for node 2, green is for node 16, red is for node 6*), (e) Number of messages arrived to each destination for the Random topology, (f) Number of messages arrived to each destination for the Scale-free topology, (g) Number of messages arrived from each source for the Grid topology (*blue is for node 14, green is for node 8, red is for node 9*), (h) Number of messages arrived from each source for the Random topology, and (i) number of messages arrived to each source for the Scale topology.

topology and 12 for Scale-free topology. We believe that one reason for this is the amount of links that differ between the three topologies, as well as lesser chance of conjugation as illustrated from Fig. 14. Therefore, due to the higher number of links, this will result in a higher number of bacteria, and hence could provide a larger number of diverse paths to connect between nodes. For example, in the Grid topology, the connectivity between nodes 16 and 14, can take two back-up paths, which are paths 16–15—14 or 16–12—11–10—14. A similar connectivity process can also be found in the Random topology where the connectivity of nodes from 14 to 2 can take paths 14–4—15–2 or 14–1—15–2. However, the number of robust backup paths in the Random topology is much less compared to the Grid topology, and this is reflected for destination node 8, where there is only a single path available. The situation gets worse in the Scale free topology, where access to and from certain nodes are only through single chemoattractant links (e.g., for nodes 9, 14, 16). As we have illustrated in the previous section, the correlation between successful arrivals of plasmids as well as successful conjugation are highest for topologies with back-up paths (e.g., Hexagon topology). The connectivity of the topology also affects the rate of conjugation that occurs, and this is shown in Fig. 16. The previous section has shown

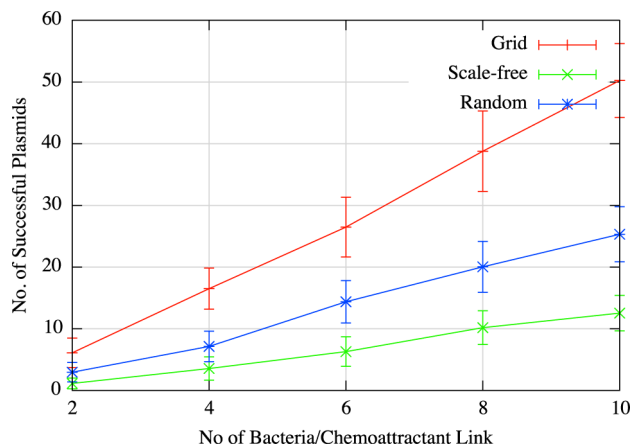

Fig. 15. Number of successful plasmids vs number of bacteria/chemoattractant link.

that the correlation $\rho(xy)$ drops when the number of disjoint paths or broken chemoattractant links lies in the topology.

Fig. 17 shows the average probability of plasmids arrival at the destination with respect to time $(P_{Arr}(t_{range}))$, for multiple simulation runs. Fig. 17(a) shows that the probability peaks at approximately time 2000 s, and starts to drop off linearly for

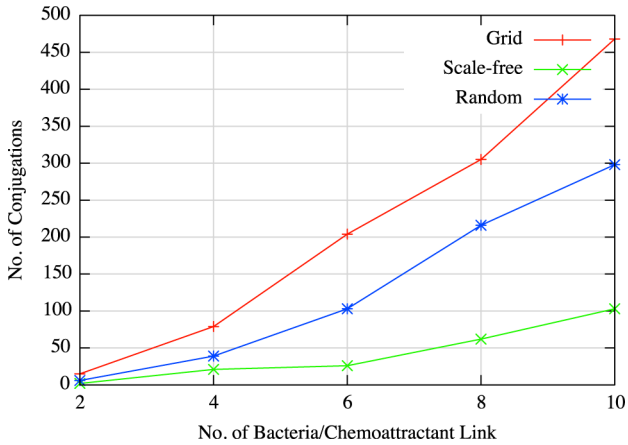

Fig. 16. Number of conjugations vs number of bacteria/chemoattractant link.

the Grid topology. The Grid topology also shows on average higher probability $P_{Arr}(t_{range})$ compared to the Random and Scale-free topologies. At time $t_{range} = 1000 - 2000$ s, we see that probability $P_{Arr}(t_{range})$ can get as high as 0.215. However, the peak of the Random topology, which occurs at time $t_{range} = 3000 - 4000$ s results in probability $P_{Arr}(t_{range})$ of only 0.145. In the case of Scale-free topology, we do get a peak at time $t_{range} = 0 - 1000$ s, where the probability $P_{Arr}(t_{range})$ gets as high as 0.21. We believe that the trend of higher probability towards the end of the simulation cycle is due to the conjugation delay (t_{conj}). However, if the duration of the simulation is longer, we see a rise in the probability towards the end of the simulation run. Fig. 17(b) shows this trend, where the probability starts to rise as the conjugation process for multiple messages completes, and more number of bacteria reaches the destination. Please note that this behavior results from the fact that the Random topology has a lower number of bacteria, and therefore, would encounter a lower number of multiple conjugation processes. A similar behavior can also be observed for the Scale-free topology [Fig. 17(c)].

Fig. 18 presents the mutual information $I(X : Y)$ for successful plasmids reaching the destination for the three topologies, where results show the mutual information before and after antibiotics were applied. As described earlier, the conjugation process can lead to situations where conjugations are not fully completed leading to portion of the message plasmids being copied to the new bacterium. This will lead to extra noise within the network, and will also lead to the recipient nanomachine requiring extra processing capabilities to filter out incomplete messages. Therefore, an alternative is to apply antibiotics to kill bacteria that do not have full messages in their plasmids. For simplicity, the simulation of the antibiotics is only conducted locally at the receiver nanomachines, by releasing the antibiotics to kill the bacteria that approach the receivers. In order to evaluate the effects of antibiotics, we simulated varying quantity of bacteria/chemoattractant links and observed the mutual information $I(X : Y)$. As we can see, the mutual information $I(X : Y)$ on average increases as we apply the antibiotics locally to clean the noise (in this case the bacteria with incomplete plasmids) for all number of bacteria/chemoattractant links. In particular, a small quantity of bacteria/chemoattractant link demonstrates the best improvements, and this is particularly the case for Grid topology (mutual information $I(X : Y)$ of 1.86 after antibiotics application compared to 1.6 before any antibiotics application) and Scale-free topology (mutual information $I(X : Y)$ of 4.6 after antibiotics application compared to 3.6 before antibiotics application). There is an improvement in mutual information $I(X : Y)$ for the Random topology with 2 bacteria/chemoattractant links, although the improvement has been minimal (mutual information $I(X : Y)$ of 0.025 before antibiotics application compared to 0.031 after antibiotics application). The mutual information $I(X : Y)$ does drop towards the higher number of bacteria/chemoattractant links, and this again is attributed to the amount of conjugations which of course leads to extra delay and prevents certain bacteria from reaching the destination nodes. This is also due to the same simulation time that is used for all the possible numbers of bacteria/chemoattractant links.

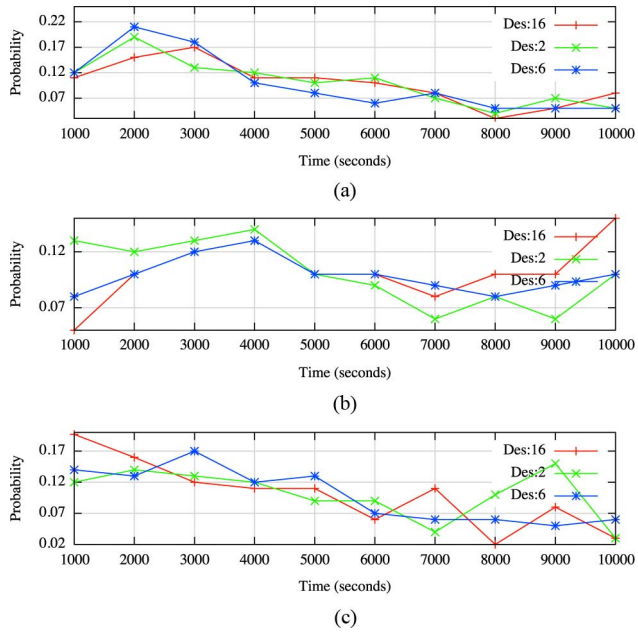

Fig. 17. Probability time of message plasmid arrival at destination $(P_{Arr}(t_{range}))$, where t_{range} is time duration) for (a) Grid, (b) Random, (c) Scale-free topologies.

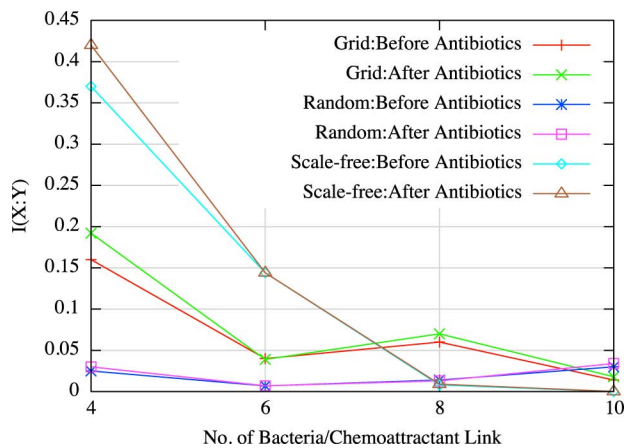

Fig. 18. Mutual information I(X:Y) comparison for antibiotics application.

TABLE IV
MAPPING OF NETWORK PROCESS TO BACTERIA PROCESS

Network Process	Bacteria process
Relaying.	Bacterium conjugation.
Corrupt packet filtering.	Antibiotics for bacteria death.
Packet structure (addressing, message).	Plasmid coding through watermarking.
DTN opportunistic based routing.	Bacteria conjugation and chemotaxis.
Message aggregation.	Multiple plasmids/bacteria.

VIII. DISCUSSION

Due to the various properties of bacteria, a number of different applications are possible, in particular for molecular computing and communications [23]. Table IV presents a summary mapping between communication networking functionalities to bacteria properties. In particular, we have focused on networking properties that we believe are essential to realize simple bacteria nanonetworks, such as addressing, routing, etc. In this section, we will describe some key applications and possible future directions that can be taken by building on the mechanisms that we have presented in this paper.

A. Micro and Nanofluidics

From a technological point of view our work fits very well to micro and nanofluidic devices. Microfluidics can be defined as the study and analysis of liquid flows within chambers that are circulating within an artificial microsystem. Our proposed approach can further advance microfluidics technology, by integrating novel bacterial fluidics. This in turn could lead to internal fluid channel networks, where bacteria can swim and carry contents between locations in the microsystems. Using the bacteria to carry contents in the channel of the microfluidic devices could eliminate the need of specific devices (e.g., pumps, gears) to control the flow of fluids in the channel. Multi-function microsystems can be implemented as a microfluidic lab-on-a-chip, which will provide a platform to conduct a variety of chemical, biological, and biomedical applications.

B. Receiver Design

While this paper has concentrated on the process of delivering plasmids from a source to a receiver nanomachine, we have not focused on how nanomachines can be designed to i) offload plasmids to bacteria to carry this towards the destination, and ii) enable bacteria to latch onto the receiver to offload plasmids to the bacteria. In order to achieve this, nanomachines will need to be designed with organic material interface that is compatible to bacteria. One possible approach could be through developing thin biofilms on the surface of the nanomachine. Biofilms are formed from aggregation of bacteria, which leads to the bacteria adhering to each other. For example, certain species of bacteria can form floating biofilms between the air/liquid interface. Therefore, through biofilms formed on the nanomachines, the carrier bacterium could latch on and perform conjugation to pick up the plasmid, and at the receiver nanomachine, the reverse process could be performed, where the bacterium can conjugate to the biofilm to pass on the plasmids. One important extension is combining a plasmid with a gene, where the gene can encode Green Fluorescent Protein (GFP). The gene that encodes the GFP is from a bacterium living in a fish, which is *Vibrio fischeri* . Through this property GFP has become widely used in research as a reporter molecule. The use of GFP could enable monitoring and quantifying conjugative plasmid transfer between bacteria. Therefore, target receiver nodes may have light sensors which will identify and detect GFP containing bacterial traffic. It is likely that future synthetic biology design techniques will provide means to improve bacteria communication nanonetworks [26].

C. Potentials in Using Antibiotics

Besides cleaning the network environment of bacteria with illegitimate plasmid messages, the antibiotics could also be utilized to control other phenomena that can occur in bacteria nanonetworks. One of these phenomena is the process of hitchhiking, which could lead to the hijacking process. Genetic hitchhiking is the process by which a gene variant may increase in frequency and get passed between bacteria. In our framework, any genetic message that is present and transferred together with the selected message could lead to possible hijacking. A typical example of hijacking is from viruses such as a *phagus* which infects the bacteria and enables transduction (i.e., introduction of new messages). Therefore, antibiotics could be used to control the behavior of bacteria, in order to avoid undesired behavior that may have resulted from genetic hitchhiking.

IX. CONCLUSION

As the field of molecular communication starts to gain traction with various physical layer solutions proposed (e.g., calcium signaling, molecular diffusion, neuronal networks), the next stage is to propose solutions that can enable molecular nanonetworking. Through molecular nanonetworking, nanomachines can perform peer-to-peer communication, which further enhances their capabilities, functionalities, as well as their application base. In this paper, we have proposed a solution for multi-hop bacteria nanonetworks. The proposed approach models the processes and mechanisms found in IP communication networks, such as opportunistic routing, packet addressing, or packet filtering, and maps these to processes found in bacteria. In particular, two main properties that we have concentrated in this paper are bacterial conjugation and chemotaxis. The simulation conducted in this paper evaluated and analyzed various multi-hop networking characteristics, such as the reliability of message delivery for different topology shapes (e.g., Grid, Random, and Scale-free) as well as the analysis on the importance of conjugation processes and its impact on plasmid delivery success rate. Our analysis has shown that our proposed approach of using properties such as chemotaxis and conjugation can be applicable to numerous topology shapes, not limited to the topologies that were used in our simulation. The paper also proposed the use of antibiotics to further improve the rate of legitimate plasmid delivery to the destination. The paper concludes with a discussion on possible extensions that can utilize multi-hop bacteria nanonetworks for future applications.

REFERENCES

[1] I. F. Akylidiz, F. Brunetti, and C. Blazquez, "Nanonetworking: A communication paradigm," *Comput. Netw.*, vol. 52, pp. 2260–2279, Jun. 2008.

[2] T. Nakano and J. Q. Liu, "Design and analysis of molecular relay channels: An information theoretic approach," *IEEE Trans. NanoBiosci.*, vol. 9, no. 3, pp. 213–221, 2010.

[3] S. Balasubramaniam, N. T. Boyle, A. Della-Chiesa, F. Walsh, A. Mardinoglu, and D. B. A. Prina-Mello, "Development of artificial neuronal networks for molecular communication," *Nano Commun. Netw.*, vol. 2, no. 2–3, Jun./Sep. 2011.

[4] L. C. Cobo-Rus and I. F. Akyildiz, "Bacteria-based communication in nanonetworks," *Nano Commun. Netw.*, vol. 1, no. 4, pp. 244–256, Dec. 2010.

[5] P. Lio' and S. Balasubramaniam, "Opportunistic routing through conjugation in bacteria communication nanonetwork," *Nano Commun. Netw.*, vol. 3, no. 1, pp. 36–45, 2012.

[6] F. C. Tenover, "Mechanisms of antimicrobial resistance in bacteria," *Amer. J. Med.*, vol. 119, 2006.

[7] C. Lagido, I. J. Wilson, L. A. Glover, and J. I. Prosser, "A model for bacterial congugal gene transfer on solid surfaces," *FEMS Microbiol. Ecol.*, vol. 44, pp. 67–2003.

[8] R. Gehring, P. Schumm, M. Youssef, and C. Scoglio, "A network-based approach for resistance transmission in bacterial populations," *J. Theor. Biol.*, vol. 262, no. 1, pp. 97–106, 2010.

[9] Y. Gao, S. Lakshmann, and R. Sivakumar, "On attractant scheduling in networks based on bacterial communication," in *Proc. IEEE Int. Workshop Mol. Nano Commun. (MoNaCom)*, Shanghai, China, 2011.

[10] Z. Wang, M. Kim, and G. Rosen, "Validating models of bacterial chemotaxis by simulating the random motility coefficient," in *Proc. 8th IEEE Int. Conf. BioInf. BioEng.*, Athens, Greece, Oct. 2008.

[11] M. J. Moore, K. Oiwa, and T. Suda, "Molecular communication: Modeling noise effects on information rate," *IEEE Trans. Nanobiosci.*, vol. 8, no. 2, pp. 169–180, Jun. 2009.

[12] G. P. Dubey and S. Ben-Yehuda, "Intercellular nanotubes mediate bacterial communication," *Cell*, vol. 144, no. 18, pp. 590–600, Feb. 2011.

[13] D. B. Dusenbery*, Living at Micro Scale: The Unexpected Physics of Being Small*. Cambridge, MA, USA: Harvard Univ. Press, 2011.

[14] B. Atakan, S. Galmes, and O. B. Akan, "Nanoscale communication with molecular arrays in nanonetworks," *IEEE Trans. NanoBiosci.*, vol. 11, no. 2, pp. 149–160, Jun. 2012.

[15] A. Guney, B. Atakan, and O. B. Akan, "Mobile ad hoc nanonetworks with collision-based molecular communication," *IEEE Trans. Mobile Comput.*, vol. 11, no. 3, pp. 353–266, Mar. 2012.

[16] D. G. Gibson, J. I. Glass, C. Lartigue, V. N. Noskov, R. Y. Chuang, M. A. Algire, G. A. Benders, M. G. Montague, L. Ma, M. M. Moodie, C. Merryman, S. Vashee, R. Krishnakumar, N. Assad-Garcia, C. Andrews-Pfannkoch, E. A. Denisova, L. Young, Z. Q. Qi, T. H. Segall-Shapiro, C. H. Calvey, P. P. Parmar, C. A. Hutchison, H. O. Smith, and J. C. Venter, "Creation of a bacterial cell controlled by a chemically synthesized genome," *Sci.*, vol. 329, no. 5987, pp. 52–6, Jul. 2010.

[17] P. Hui, J. Crowcroft, and E. Yoneki, "Bubble rap: Social-based forwarding in delay tolerant networks," in *Proc. 9th ACM Int. Symp. Mobile Ad Hoc Netw. Comput. (MobiHoc)*, Hong Kong, China, 2008.

[18] P. Hui, A. Chaintreau, R. Gass, J. Scott, J. Crowcroft, and C. Diot, "Pocket switched networking: Challenges, feasibility, and implementation issues," in *Proc. 2nd IFIP Autonomic Commun.*, Athens, Greece, Oct. 2005.

[19] K. D. Young, "The selective value of bacterial shape," *Microbiol. Mol. Biol. Rev.*, vol. 70, no. 3, pp. 660–703, Sep. 2006.

[20] H. C. Berg and E. M. Purcell, "Physics of chemoreception," *Biophys. J.*, vol. 20, pp. 93–219, 1977.

[21] W. Bialek and S. Setayeshgar, "Physical limits to biochemical signaling," *Proc. Natl. Acad. Sci.*, vol. 102, pp. 10040–10045, 2005.

[22] B. Suna, J. Lembongb, V. Normandc, M. Rogersc, and H. A. Stone, "Spatial-temporal dynamics of collective chemosensing," *Proc. Natl. Acad. Sci.*, vol. 109, no. 20, May 2012.

[23] J. Bonnet, P. Subsoontorn, and D. Endy, "Rewritable digital data storage in live cells via engineered control of recombination directionality," *Proc. Natl. Acad. Sci.*, May 2012.

[24] M. Gregori and I. F. Akyildiz, "A new nanonetwork architecture using flagellated bacteria and catalytic nanomotors," *IEEE J. Sel. Areas Commun.*, vol. 28, no. 4, pp. 612–619, May 2010.

[25] A. W. Bauer, D. M. Perry, and W. M. M. Kirby, "Single disc antibiotic sensitivity testing of staphylococci," *Archives Internal Med.*, vol. 104, no. 2, pp. 208–216, 1959.

[26] J. Costanza, G. Carapezza, C. Angione, P. Lio', and G. Nicosia, "Robust design of microbial strains," *Bioinformatics*, vol. 28, no. 23, 2012.

[27] M. Pierobon and I. F. Akyildiz, "A physical end-to-end model for molecular communication in nanonetworks," *IEEE J. Sel. Areas Commun.*, vol. 28, no. 4, pp. 602–611, May 2010.

[28] M. Pierobon and I. F. Akyildiz, "Diffusion-based noise analysis for molecular communication in nanonetworks," *IEEE Trans. Signal Process.*, vol. 59, no. 6, pp. 2532–2547, Jun. 2011.

[29] M. Pierobon and I. F. Akyildiz, "Noise analysis in ligand-binding reception for molecular communication in nanonetworks," *IEEE Trans. Signal Process.*, vol. 59, no. 9, pp. 4168–4182, Sep. 2011.

Authors' photographs and biographies not available at the time of publication.